ISSN 0735-1097/04/$30.00
doi:10.1016/j.jacc.2004.06.057

Identification of Less-Irradiating Tube Angulations in Invasive Cardiology

Eberhard Kuon, MD,* Johannes B. Dahm, MD,† Klaus Empen, MD,† Daniel M. Robinson, MD,† Gereon Reuter, MD,* Michael Wucherer, PHD‡
Ebermannstadt, Greifswald, and Nuremberg, Germany

OBJECTIVES We sought to identify tube angulations in invasive cardiology, which promise minimal radiation exposure to patients and operators.

BACKGROUND Radiation exposure in invasive cardiology is high.

METHODS We mapped the fluoroscopic dose-area product per second (DAP/s), applied to an anthropomorphic Alderson-Rando phantom and, in absence of radiation protection devices, the mean personal dose in the operator's position in 10° steps from the 100° right anterior oblique (RAO) to the 100° left anterior oblique (LAO) projection, as well as for all geometrically feasible craniocaudal tube angulations.

RESULTS For our specific setting conditions RAO 20°/0° tube angulation generated the lowest DAP/s and operator's personal dose. The mean patient DAP/s and operator personal dose for all postero-anterior (PA) projections, cranialized and caudalized together, rose significantly: 3.7 and 10.6 times the PA 0° baseline values toward LAO 100° and 3.7 and 2.4 times toward RAO 100°, respectively. Patient and operator values for all PA projections, angulated to the right and left, increased ~2.5 times toward 30° craniocaudal angulations. Caudal PA 0°/30°− angulation instead of caudal LAO 60°/20°− angulation for the left coronary main stem and cranial PA 0°/30°+ view in place of cranial LAO 60°/20°+ view for the left anterior descending coronary artery bifurcation enable 2.6-fold dose reductions to the patient and eight- and five-fold dose reductions to the operator, respectively.

CONCLUSIONS The PA views and RAO views ≥40°, heretofore unconventional in clinical routine, should be favored over steep LAO projections ≥40° whenever possible. Tube angulations that are radiation intensive to the patient exponentially increase the operator's radiation risk. (J Am Coll Cardiol 2004;44:1420–8) © 2004 by the American College of Cardiology Foundation

Typical mean patient dose-area products (DAP) due to coronary procedures are high and vary extensively with levels between 4 and 106 Gy × cm^2 for coronary angiography, between 8 and 109 Gy × cm^2 for coronary intervention, and between 70 and 191 Gy × cm^2 for combined interventions (1–8). Deterministic radiation risks, such as those leading to chronic radiodermatitis and deep skin and musculocutaneous injury (9,10), have been increasingly reported in conjunction with complex coronary interventions. Additionally, published data on mean entrance skin doses to the operator's unprotected eyes, thyroid, and hands are considerable and range between 120 and 400 μSv, 390 μSv, and 240 to 510 μSv per coronary intervention, respectively (11,12). Operators in a high-volume catheterization laboratory with a cumulative workload of 1,000 invasive catheterizations for stray radiation accordingly may reach and even exceed the recommended occupational yearly limits of 150 mSv for the lens of the eye, 300 mSv for the thyroid, and 500 mSv for the skin, hands, and feet (13,14). With good reason, the International Commission on Radiological Protection therefore states that "... many interventionists are not aware of the potential for injury from procedures, their occurrence, or simple methods for decreasing their incidence utilising dose control strategies" (15).

Patient radiation exposure in invasive cardiology depends on obesity (5), equipment performance (7,16), picture-quality respective image intensifier entrance dose level (17), procedure complexity (8,18), operator fatigue (19), training and supervision in radiation-reducing techniques (5,20), and correct beam collimation (5,21), and it will increase due to high-resolution magnification (5,22). In consideration of the inverse-square law between the source and the radiation intensity, accepted regulations require a minimum distance to the patient's skin of 38 cm (23). Keeping the image intensifier as close to the patient as possible minimizes the source-to-image distance (SID), which results in a decreased blurring of the image, and also allows the image intensifier to serve as a barrier between the patient and operator (23). The operator's occupational exposure also depends on an adequate use and acceptance of lead protection devices (11,24–26), case load, and distance from the isocenter (22). Doubling the source-to-operator distance (SOD) will likewise decrease the primary stray radiation scattered from the patient to approximately one quarter of the original occupational dose (27). Optimized interventional techniques (5,7,24) in clinical routine, however, have enabled mean DAPs of 4.2 ± 1.6 Gy × cm^2 for elective coronary angiography (7) and 7.8 ± 6.1 Gy × cm^2 for coronary angioplasty (8).

Tube angulation influences patient (5,17) and occupational operator radiation exposure (24,25,28,29) to an ex-

From the *Department of Cardiology, Klinik Fraenkische Schweiz, Ebermannstadt; †Department of Cardiology, Ernst-Moritz-Arndt University, Greifswald; and ‡Institute of Medical Physics, Clinic of Nuremberg, Nuremberg, Germany.

Manuscript received April 13, 2004; revised manuscript received June 6, 2004, accepted June 22, 2004.

Abbreviations and Acronyms

DAP/s = dose-area product per second
LAD = left anterior descending coronary artery
LAO = left anterior oblique
PA = postero-anterior
RAO = right anterior oblique
SID = source-to-image distance
SOD = source-to-operator distance

tensive degree (i.e., left anterior oblique [LAO] projections are most radiation intensive). Such data reported to date, however, cover only a small number of selected angulations favored by individual operators in experimental approaches or in clinical routine. They have not heretofore represented the wide range of tube angulations feasible in invasive cardiology.

For this reason, the goal of this experimental study on a male anthropomorphic Alderson-Rando phantom (Fig. 1) was to map, during fluoroscopy, for all tube angulations technically feasible in invasive cardiology, the DAP/s, applied to the phantom, and the respective local personal operator dose per time and per DAP. Such mapping, not previously described, would represent an effective tool for identification of angiographic projections that promise a significant reduction of radiation exposure in clinical routine to patients and staff. Our secondary objective was to investigate the conflict of interest, arising from the fact that the operator's scatter radiation dose does not vary as a strict function of the change in patient DAP owing to tube angulation (22,26,28).

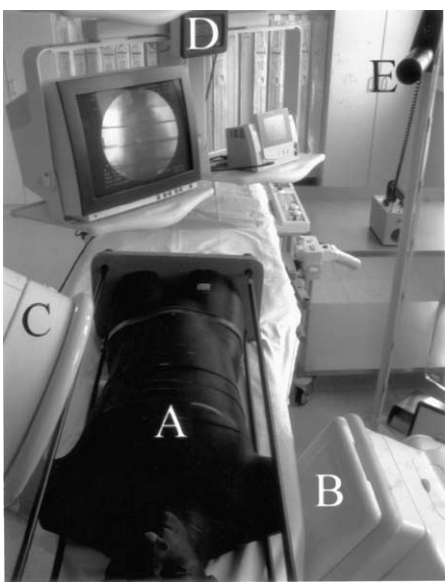

Figure 1. Catheterization laboratory with an Alderson-Rando phantom **(A)** simulating the patient: position of the tube **(B)** in undercouch and the image intensifier **(C)** in overcouch 60°/0° left anterior oblique position. The Diamentor M4 display **(D)** and the Szintomat 6134 A system **(E)** were used to measure fluoroscopic dose-area product, applied to the phantom, and the operator's personal dose.

METHODS

Equipment. We employed a digital, single-arm Advantx LC+ undercouch tube system (GE Medical Systems, Fairfield, Connecticut) with the following installed in the X-ray beam: a 0.1-mm copper filter, a 2.9-mm aluminum filter, and, throughout all measurements, an antiscatter grid. For all fluoroscopy mode levels—high, medium, and low—the pulse rate is 50/s. However, to reduce radiation exposure to the investigator, throughout all experimental measurements, we consistently applied low-level fluoroscopy, which is achieved by a lower dose per frame. Under conditions of a focus-image intensifier distance of 1 m, and for a 2-mm thick copper absorber, an automatic dose-control algorithm regulated the image intensifier entrance dose rates during low-level fluoroscopy toward 0.21 and 0.30 μGy/s for the 23- and 17-cm image intensifier area, respectively. During cine acquisition, the entrance-exposure rate was calibrated to 0.08 μGy/frame (23-cm area; mode B of four different cine acquisition modes: A, B, C, and D). We measured the DAP by a flat, light-transparent ionization Diamentor M4 (PTW, Freiburg, Germany; total uncertainty <15%).

Characterization of in vivo conditions by an Alderson-Rando phantom. The first step of methodology was to validate the assessment of DAP obtained with the phantom as compared with that received by patients (body mass index 27.9 ± 4.0 kg/m^2) in an analysis of 122 coronary angiograms. The mean patient's cinegraphic DAP/frame (17-cm intensifier field, cine acquisition mode B) obtained with the phantom versus that received by patients and measured in vivo did not differ significantly (i.e., 21.6 ± 7.7 vs. 24.0 ± 7.6 mGy × cm^2, respectively; $p > 0.38$). On the basis of straight-line regression, the correlation coefficient between the two methodological approaches for all various tube angulations was 0.91 (24,25).

The second step was to correlate stray radiation to the operator to the DAPs measured on the phantom. The correlation coefficient was 0.99 between a scattered dose at the operator's position and DAP in the 0°/0° postero-anterior (PA) tube angulation at a table height of 95 cm and a dosimeter height of 100 cm at a distance of 100 cm from the isocenter (24). In concurrence with other investigators, the operator's personal dose/DAP slightly increased with kilovolt and field size (29,30).

Data collection. We measured the low-level fluoroscopic DAP over the course of 60 s, applied to an anthropomorphic Alderson-Rando phantom for simulation of in vivo conditions (Fig. 1). At an operator's position 100 cm from the isocenter (on the right side of the patient, 60 cm adjacent to and 80 cm caudal to the tube), we then measured scattered personal dose to the operator, which is defined as the sum of primary scatter emitted from the patient in all directions, secondary scatter from the walls, and the small fraction of tube-housing leakage (23). The unit of measurement is Sievert (Sv). We performed measurements in 20-cm increments within a height range of 20 to 200 cm (10

Table 1. Time-Adjusted Radiation Exposure (mGy × cm²/s) to an Alderson-Rando Phantom in Dependency on Tube Angulation*

	RAO										PA	LAO									
	100°	**90°**	**80°**	**70°**	**60°**	**50°**	**40°**	**30°**	**20°**	**10°**	**0°**	**10°**	**20°**	**30°**	**40°**	**50°**	**60°**	**70°**	**80°**	**90°**	**100°**
Cranial																					
40°							43	54	44	47	50	57	71	80							
30°	94	89	58	33	31	32	31	**29**	**25**	**23**	**19**	**29**	**34**	46	67	75	84	82	106	111	133
20°	53	49	34	29	25	24	24	**19**	**18**	**18**	**17**	**22**	**25**	**28**	**34**	**43**	**49**	51	52	79	85
10°	35	33	28	26	23	22	19	**17**	**14**	**14**	**13**	**17**	**20**	**35**	**24**	**31**	**38**	**35**	**36**	**39**	48
PA																					
0°	30	31	27	26	24	23	16	**13**	**12**	**12**	**13**	**16**	**17**	**19**	**19**	**30**	**31**	**29**	**27**	**28**	**29**
Caudal																					
10°	37	47	46	44	32	30	21	**16**	**13**	**12**	**12**	**18**	**18**	**21**	**24**	**38**	**42**	**43**	**33**	**28**	30
20°	50	70	81	69	66	41	28	**21**	**15**	**15**	**15**	**20**	**23**	**23**	**31**	**49**	**61**	63	55	41	39
30°	83	102	108	84	78	44	25	**23**	**18**	**22**	**23**	**32**	**31**	34	38	55	81	98	94	89	58
40°							80	33	24	36	40	49	51	55	57						

*Boldface characters indicate range of typically used tube angulations.
LAO = left anterior oblique; PA = posteroanterior; RAO = right anterior oblique.

positions) with a Szintomat 6134 A system (Automess, Ladenburg, Germany). The system was calibrated for a dose intensity range of 100 nSv/h to 100 mSv/h (total uncertainty <10%).

The fluoroscopic DAP/s (Table 1, Fig. 2) and the respective mean personal operator doses/h (Table 2, Fig. 3) were measured and calculated in 10° steps for all tube angulations from RAO 100° to LAO 100°. We investigated these 21 different angulations around the phantom and the table not only for the plane at right angles (PA 0°) to the phantom, but also in repetition for planes angulated cranially (+) and caudally (−) by 10°, 20°, and 30°. We also performed measurements for 40°, unless rendered unfeasible by the geometric setting circumstances. We accordingly performed for 164 ([21 × 7] + 17) individual tube angulations measurements of fluoroscopic DAP/s and a total of 1,640 (164 × 10) local measurements of operator dose. We finally calculated the operator's mean personal dose per DAP, applied to the Alderson-Rando phantom (Table 3). Primary and secondary scatter radiation depends directly on DAP, applied to the phantom. However, DAP depends on tube angulation. The personal dose to DAP ratio enables characterization of the additional occupational operator stray radiation risk due to certain tube angulations (26).

RESULTS

Phantom radiation exposure. Fluoroscopic DAP/time was lowest (12 mGy × cm²/s) for the RAO 20°/0° tube angulation and highest (31 mGy × cm²/s) toward the lateral LAO 60°/0° and RAO 90°/0° angulations (Table 1,

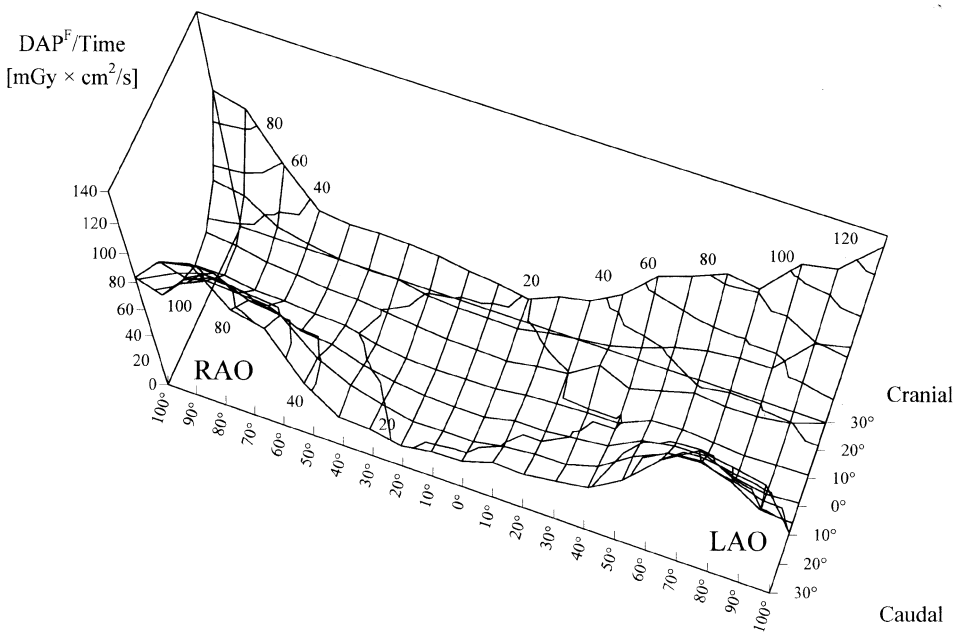

Figure 2. Calculated isodose lines in a three-dimensional graph of time-adjusted fluoroscopic dose-area product (DAP) (DAP^F/time [mGy × cm²/s]), as a function of tube angulation. LAO = left anterior oblique; RAO = right anterior oblique.

Table 2. Mean Operator Radiation Exposure (μSv/h) During Fluoroscopy at a Rando Phantom as a Function of Tube Angulation*

	RAO								PA	LAO							
	100°	**90°**	**80°**	**70°**	**60°**	**50°**	**40°**	**30°**	**20°**	**10°**	**0°**	**10°**	**20°**	**30°**	**40°**	**50°**	**60°**	**70°**	**80°**	**90°**	**100°**
Cranial																					
40°							280	490	420	460	420	510	650	790							
30°	500	390	250	140	120	140	200	**230**	**210**	**210**	**200**	**240**	**290**	440	770	1,100	1,300	1,400	1,700	1,800	2,200
20°	280	260	200	130	110	140	160	**140**	**150**	**160**	**150**	**190**	**240**	**310**	**390**	**660**	**1,000**	1,200	1,400	2,100	2,100
10°	210	200	170	120	120	140	130	**120**	**120**	**110**	**110**	**160**	**220**	**290**	**350**	**560**	**800**	**880**	**890**	**960**	1,200
PA																					
0°	190	190	170	160	150	120	100	**80**	**80**	**90**	**100**	**150**	**180**	**250**	**290**	**600**	**730**	**690**	**650**	**630**	**640**
Caudal																					
10°	250	280	270	230	200	200	140	**120**	**100**	**110**	**110**	**190**	**210**	**270**	**390**	**750**	**1,100**	**1,100**	**820**	**670**	670
20°	350	410	480	360	320	270	190	**150**	**110**	**120**	**130**	**250**	**260**	**300**	**490**	**910**	**1,600**	1,800	1,500	1,000	850
30°	320	480	530	300	290	240	140	**140**	**140**	**180**	**210**	**320**	**350**	440	500	860	1,800	2,300	2,500	2,400	1,400
40°							590	200	160	310	360	470	550	680	700						

*Boldface characters indicate range of typically used tube angulations. Abbreviations as in Table 1.

Figure 3. Calculated isodose lines in a three-dimensional graph of the operator's mean personal dose per time (μSv/h), as a function of tube angulation. LAO = left anterior oblique; PA = posteroanterior; RAO = right anterior oblique.

Fig. 2). The mean radiation exposure values for all craniocaudal tube angulations along the table (cranial 0°/30°+ to caudal 0°/30°− projection) continuously rose to ~3.7 times that of the PA baseline values toward both the respective mean RAO 100° and LAO 100° angulation planes. The mean radiation exposure values for all 21 tube angulations at right angles around the phantom (RAO 100°/0° to LAO 100°/0° projection) continuously rose to ~2.6 times that of the baseline values toward 30° craniocaudal angulation planes. Further craniocaudal tube angulation toward an angle of 40° creates even more radiation exposure to the phantom. Consequently, fluoroscopic DAP/time is highest for extreme oblique tube angulations ≥50°, which are angulated ≥20° toward cranial and caudal, respectively (Fig. 2, Table 1).

Operator occupational dose. The mean local scatter dose in the operator position—measured from 20 to 200 cm body height—was lowest for the RAO 20°/0° tube angulation: 80 μSv/h. It increased to mean peak levels of 730 μSv/h toward LAO tube angulations between 50°/0° and 100°/0° (Table 2, Fig. 3) and of 190 μSv/h toward the RAO 90°/0° tube angulation. The operator's mean personal dose during fluoroscopy of all seven tube angulations along the table between cranial 30°+ and caudal 30°− continuously rose to ~10.6 times PA baseline values toward the LAO 90° tube

Table 3. Dose-Corrected Operator Scatter Exposure (μSv/Gy × cm^2) During Fluoroscopy as a Function of Tube Angulation*

	RAO									PA	LAO								
	100°	**90°**	**80°**	**70°**	**60°**	**50°**	**40°**	**30°**	**20°**	**10°**	**0°**	**10°**	**20°**	**30°**	**40°**	**50°**	**60°**	**70°**	**80°**	**90°**	**100°**
Cranial																					
40°							1.8	2.5	2.7	2.7	2.3	2.5	2.5	2.7							
30°	1.5	1.2	1.2	1.2	1.1	1.3	1.8	**2.2**	**2.3**	**2.5**	**2.9**	**2.3**	**2.4**	2.7	3.2	4.0	4.3	4.9	4.5	4.5	4.6
20°	1.5	1.5	1.6	1.2	1.2	1.6	1.8	**2.0**	**2.3**	**2.5**	**2.5**	**2.4**	**2.7**	**3.1**	**3.2**	**4.3**	**6.0**	6.5	7.3	7.4	7.0
10°	1.7	1.7	1.8	1.4	1.5	1.8	1.9	**2.0**	**2.2**	**2.2**	**2.4**	**2.7**	**3.2**	**2.3**	**4.0**	**5.1**	**5.9**	**6.9**	**6.9**	**6.7**	6.8
PA																					
0°	1.7	1.7	1.8	1.6	1.7	1.5	1.7	**1.9**	**2.0**	**2.0**	**2.3**	**2.6**	**2.9**	**3.7**	**4.3**	**5.5**	**6.5**	**6.5**	**6.6**	**6.2**	**6.2**
Caudal																					
10°	1.9	1.6	1.7	1.4	1.7	1.9	1.8	**2.0**	**2.2**	**2.4**	**2.4**	**3.0**	**3.2**	**3.6**	**4.6**	**5.6**	**7.0**	**7.3**	**6.9**	**6.6**	6.1
20°	1.9	1.6	1.6	1.4	1.4	1.8	1.9	**2.0**	**2.1**	**2.2**	**2.4**	**3.4**	**3.2**	**3.7**	**4.3**	**5.2**	**7.4**	8.0	7.7	6.8	6.0
30°	1.1	1.3	1.4	1.0	1.0	1.5	1.6	**1.7**	**2.1**	**2.3**	**2.5**	**2.8**	**3.2**	3.6	3.6	4.4	6.2	6.4	7.4	7.4	6.6
40°							2.0	1.7	1.8	2.3	2.5	2.6	3.0	3.4	3.4						

*Boldface characters indicate range of typically used tube angulations.
Abbreviations as in Table 1.

Figure 4. Ostial lesion of the left coronary main stem **(arrowhead):** cranial posteroanterior (PA) 0°/30°+ and PA 0°/0° angulations enable personal dose levels much lower than those obtained with the typical caudal left anterior oblique (LAO) 60°/20°− angulation.

angulation and merely to 2.4 times toward the RAO 90° angulation. The mean radiation exposure values for all 21 tube projections in the plane at right angles around the phantom continuously rose up to ~2.4 times toward 30° craniocaudal angulations. Scatter radiation to the operator during fluoroscopy is consequently highest—up to 2,500 μSv/h—in extreme diagonal LAO tube angulations (Fig. 3, Table 2).

In Tables 1 and 2, we have highlighted in boldface the data for radiation exposure produced by the range of tube angulations typically used in clinical routine. A typical standard view for the left coronary main stem is the caudal LAO 60°/20°− angulation (Fig. 4), which, however, generates a 2.6-fold increase in the DAP/s level and a 7.6-fold increase in the operator radiation level from caudal PA 0°/30°− angulation, respectively. Documentation of an ostial lesion of the left coronary main stem in the cranial PA 0°/30°+ and PA 0°/0° angulation will likewise significantly reduce the patient and operator dose to even lower levels (Figs. 2, 3, and 4, Tables 1 and 2). The same applies to the typical cranial LAO 60°/20°+ angulation for visualization of the bifurcation into the left anterior descending coronary artery (LAD) and diagonal artery. This angulation in comparison to the cranial PA 0°/30°+ view produces a 2.5-fold increase in DAP/s to the phantom and a fivefold

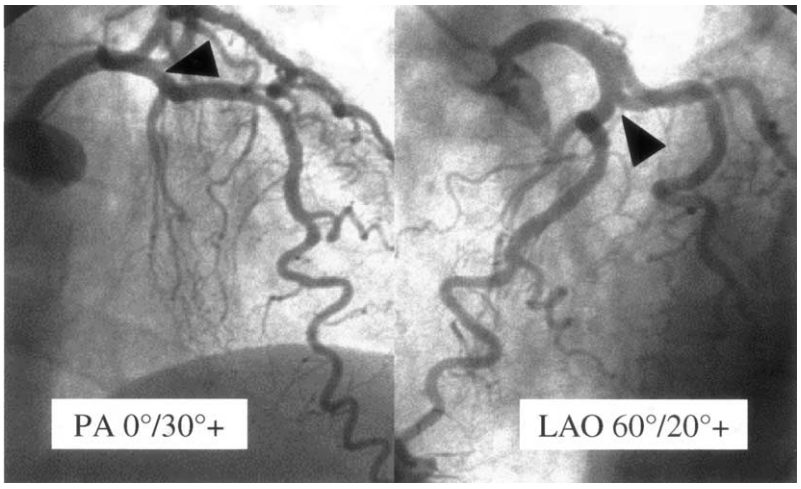

Figure 5. Bifurcation **(arrowheads)** into the left anterior descending and diagonal artery: cranial posteroanterior (PA) 0°/30°+ enables operator dose levels considerably lower than those obtained with the typical cranial left anterior oblique (LAO) 60°/20°+ angulation.

increase in the scatter radiation dose level to the operator (Fig. 5, Tables 1 and 2). Neither of these unconventional angulations are, to be sure, typically practiced in invasive cardiology. For the same reason, the RAO 30°/0° angulation should be favored over the cranial RAO 30°/30°+ angulation for documentation of the LAD.

The ratio between the mean scatter radiation dose in the operator position and the DAP applied to the phantom characterizes the particular additional occupational operator stray radiation risk for certain radiation intensive tube angulations (Table 3). It significantly increases to three- to fourfold levels toward steep LAO angulations, owing to the considerable backscatter radiation from the patient's right side toward the operator, up to 8.0 μSv/Gy $\times$ cm^2 for the caudal LAO 70°/20°− tube angulation. Conversely, in efforts toward operator radiation protection, the RAO 90°/0° angulation enables much lower operator radiation

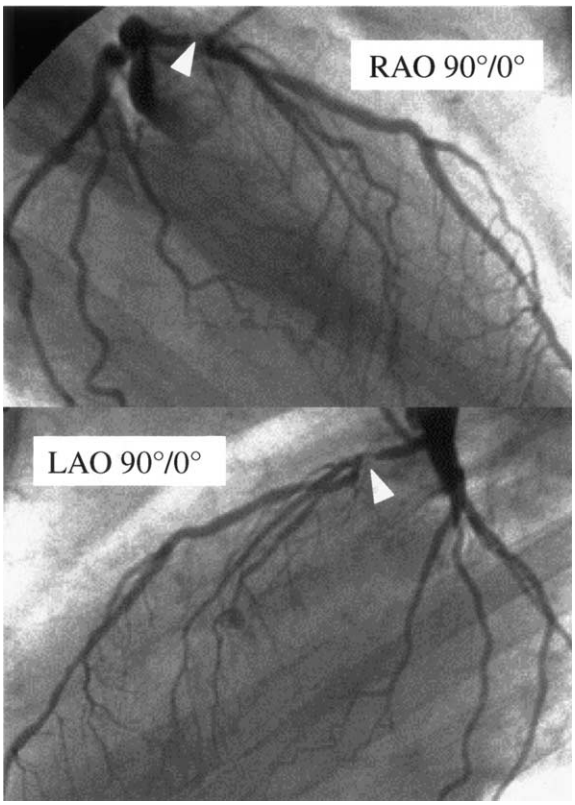

Figure 6. The left anterior descending artery lesion **(arrowhead):** right anterior oblique (RAO) 90°/0° angulation enables operator dose levels significantly lower than those obtained with the typical left anterior oblique (LAO) 90°/0° view.

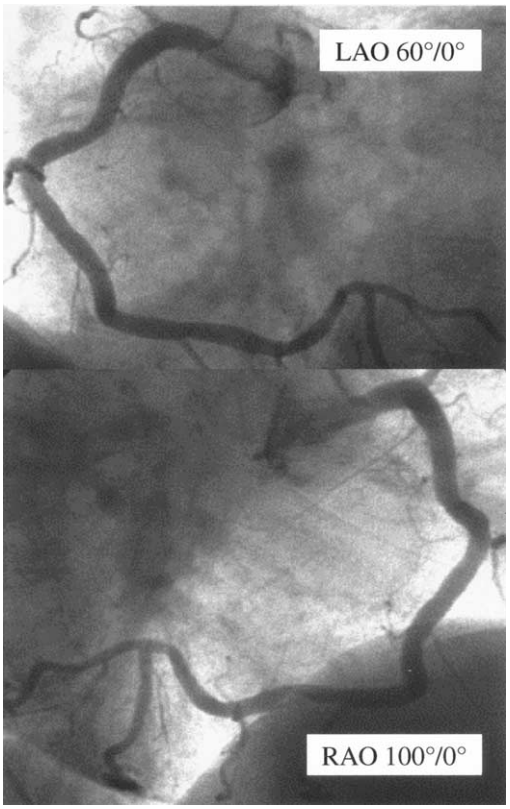

Figure 7. Right coronary artery: right anterior oblique (RAO) 100°/0° angulation enables operator dose levels significantly lower than those obtained the typical left anterior oblique (LAO) 60°/0° view.

Table 4. Occupational Operator Dose Reduction by Less Irradiating Tube Angulations in Invasive Cardiology

Target Structure	Typical Angulation	Recommended Angulation	Dose Reduction (%)	
			Patient (Table 1)	Operator (Table 2)
Left ventricle	LAO 60°/0°	LAO 40°/0°	−40	−60
	LAO 60°/0°	RAO 100°/0°	−2	−74
Left main stem bifurcation	LAO 60°/20° − (caudal)	PA 0°/30° − (caudal)	−62	−87
Left main stem orifice	LAO60°/20° − (caudal)	PA 0°/30° + (cranial)	−69	−88
Left main stem	LAO 60°/20° − (caudal)	PA 0°/0°	−79	−94
LAD panoramic view	LAO 90°/0°	RAO 90°/0°	+9	−70
Mid/peripheral LAD	RAO 30°/30° + (cranial)	RAO 30°/0°	−57	−63
LAD/D bifurcation	LAO 60°/20° + (cranial)	PA 0°/30° + (cranial)	−60	−81
Cx	LAO 60°/0°	RAO 10°/30° − (caudal)	−28	−75
RCA	LAO 60°/0°	LAO 30°/0°	−40	−66
RCA	LAO 60°/0°	RAO 100°/0°	−2	−74

+ = cranial; − = caudal; Cx = circumflex artery; D = diagonal artery; LAD = left anterior descending coronary artery; RCA = right coronary artery.

exposure than does the typical LAO 90°/0° view (i.e., the LAD will be documented 180° around the patient), without any loss of diagnostic information (Fig. 6). Furthermore, RAO angulations ≥40° enable very low absolute and DAP-corrected operator radiation exposure levels (Tables 2 and 3). It is, however, precisely these angulations that are unconventional in clinical routine (Fig. 7).

DISCUSSION

This study clearly reveals that mapping of the time-adjusted fluoroscopic DAP, applied to an Alderson-Rando phantom, and of mean personal dose in the operator's position, in accordance with all tube angulations feasible in invasive cardiology, enables identification of projections for coronary procedures that in clinical routine promise significant reduction of radiation exposure to patients and staff.

Tube angulation, likewise, considerably influences patient and operator radiation exposure in invasive cardiology (i.e., steep LAO tube angulations are most radiation intensive for the patient [5,17,24] and operator [24,25,28]). These data, however, cannot be considered representative. Indeed, favored tube angulations for special investigations in invasive cardiology vary extensively among catheterization laboratories and even among experienced individual operators. For the first time, the present experimental approach (i.e., mapping the time-corrected fluoroscopic DAP and time-corrected mean personal operator dose for each conceivable tube angulation) provides a representative and valuable data tool for every interventionist to examine the possibility of less radiation-intensive angulations in clinical routine.

In the context of this objective, the few existing clinical studies corroborate our experimental setting. Employing the caudal RAO 10°/30°− instead of the former LAO 60°/0° view reduced the fluoroscopic operator dose by 75%, a level obtained by averaging readings from five body points (eye, thyroid, chest, gonads, and knees). Additionally, a 43% reduction was seen by favoring the LAO 30°/0° over the LAO 45°/0° angulation for percutaneous transluminal coronary angioplasty of the left circumflex and right coronary artery (28). The dose reductions derived by simulation of these improved angulations in our experimental approach were highly comparable (i.e., 75% and 44%, respectively). Furthermore, in accordance with the aforementioned experimental results, our previous clinical data have shown that the cranial RAO 30°/30° angulation for exact documentation of the right coronary bifurcation at the crux occasions greater radiation intensity than does the RAO 30°/0° view (5,17).

The present analysis disclosed numerous additional details (Table 4). Interventionists, for example, should avoid the typical caudal LAO spider view for documentation of the left main stem, in favor of the cranial PA view for its proximal region and the caudal PA view for its distal bifurcation. The panoramic lateral RAO 90°/0° view of the LAD allows significant radiation benefits over the typical LAO 90°/0° projection (Fig. 6). For its mid and peripheral segments, the RAO 30°/0° angulation should be favored over the cranial RAO 30°/30° angulation. For example, fluoroscopy in the course of a percutaneous coronary intervention of the bifurcation into the LAD and diagonal artery (Fig. 5) in the PA cranial 0°/30°+ view for 49 s will provide the same exposure as the cranial LAO 60°/20°+ angulation for 19 s (Table 1). It is evidently meaningful to establish left ventriculography in the LAO 40°/0° or, even more effective in reducing operator stray radiation, in the steep lateral RAO 100°/0° instead of the LAO 60°/0° angulation for assessment of septal and lateral wall motion. The same applies for documentation of the right coronary main stem up to the crux and the right posterolateral branch (Fig. 7). From the viewpoint of radiation protection of patients and staff, interventionists should avoid steep LAO tube angulations whenever possible. The LAO views ≥60° with cranial or caudal angulation ≥20° are unjustifiable and obsolete; it is precisely those views which imply a longer SID and, consequently, more radiation exposure to patients and staff. From the viewpoint of interventional routine, however, the best views are those that demonstrate the particular coronary lesion with the least overlap of other structures and in its "worst stenosis" view. If some radiation intensive angulations are unavoidable, the interventionist should, as far as

possible, minimize lengthy cinegraphic documentation and should increase the SOD.

Another topic needs to be discussed. Given the inverse-square law, any experienced interventionist will wonder why the caudal LAO view results in as much occupational radiation exposure as the cranial LAO view. The logical explanation might be as follows: while caudalization of angulation indeed will cranially distance the undercouch tube as well as the patient's skin entrance site from the operator position, the operator dose will nevertheless not decrease, for a greater proportion of the scatter radiation will be directed from that entrance site caudally toward him or her.

A few limitations of our experimental approach are worthy of mention. Firstly, our conclusions in their quantitative aspects are dependent on the X-ray system used and its setting in a particular center. Secondly, it is not possible to transfer our data on patient exposure during angiography of the right coronary artery without reservation; because for this vessel, it is difficult to identify PA and RAO projections that rotate out the spine. Not least, our experimental approach recorded an over-apron operator radiation dose in the course of invasive cardiac procedures without table-attached and personal radiation protection devices. With use of 0.5- and 1.0-mm overcouch and undercouch shielding, it was possible to reduce the mean operator radiation exposure to 14% and 6% of baseline, respectively. Closure of radiation leakage at 80 to 105 cm of height was achieved by an additional 1.0-mm lead-equivalent undercouch-top and overcouch-flap, adjacent to the table, and resulted in a reduction of radiation exposure levels down to 1% of baseline. Such new, state-of-the-art table-attached lead protection enabled fluoroscopic radiation exposure levels in the operator's position from 3 (PA 0°/0°) to 16 μSv/h (caudal LAO 60°/20°−) and from 60 to 180 nSv/h above and beneath 0.5-mm lead apron, collar, glasses, helmet, and foot-switch shield (24,25). Baseline levels for these reference angulations were 100 and 1,600 μSv/h, respectively. In consequence, the better fixed and personal radiation protection devices are, the less important will be tube angulation with respect to operator radiation exposure. In clinical routine, however, as emphasized recently, measured occupational over-apron doses differed due to the irregular use of thermoluminescence dose meters and film badges (21), and the protective overcouch screen was, "when used, . . . appropriate only occasionally" (11).

The present experimental approach provides the first available mapping of the DAP-corrected mean local scatter dose to the operator for each conceivable tube angulation and offers a representative data tool for every cardiology interventionist to check his or her own occupational radiation risk resulting from favored coronary views and to find less radiation-intensive angulations. Furthermore, our data definitively rule out any conflict of interest between radiation protection of the patient versus operator and staff. The operator's personal dose due to scatter radiation fundamentally correlates with the patient's DAP variability resulting from tube angulation. Tube angulations that are radiation intensive to the patient, moreover, multiply the radiation risk for the operator and staff. In conclusion, the present study on identification of less-irradiating angulations supports a reassuring message to the interventional cardiology community: what's good for our patients will be even better for ourselves.

Reprint requests and correspondence: Dr. Eberhard Kuon, Klinik Fraenkische Schweiz, Feuersteinstr. 2, D-91320 Ebermannstadt, Germany. E-mail: Eberhard.Kuon@klinik-fraenkische-schweiz.de.

REFERENCES

1. Katritsis D, Efstathopoulos E, Betsou S, et al. Radiation exposure of patients and coronary arteries in the stent era: a prospective study. Cathet Cardiovasc Interv 2000;51:259–64.
2. Van de Putte S, Verhaegen F, Taeymans Y, Thierens H. Correlation of patient skin doses in cardiac interventional radiology with dose-area product. Br J Radiol 2000;73:504–13.
3. Arthur WR, Dhawan J, Norell MS, Hunter AJ, Clark AL. Does cardiologist- or radiographer-operated fluoroscopy and image acquisition influence optimization of patient radiation exposure during routine coronary angiography? Br J Radiol 2002;75:748–53.
4. Neofotistou V, Vano E, Padovani R, et al. Preliminary reference levels in interventional cardiology. Eur Radiol 2003;13:2259–63.
5. Kuon E, Glaser C, Dahm JB. Effective techniques to reduce radiation dosage to patients undergoing invasive cardiac procedures. Br J Radiol 2003;76:406–13.
6. Larrazet F, Dibie A, Philippe F, Palau R, Klausz R, Laborde F. Factors influencing fluoroscopy time and dose-area product values during ad hoc one-vessel percutaneous coronary angioplasty. Br J Radiol 2003;76:473–7.
7. Kuon E, Schmitt M, Dorn C, Dahm JB. Predialing the number of cinegraphic frames enables an effective patient dose due to invasive coronary angiography of 0.8 millisievert. Rofo Fortschr Geb Rontgenstr Neuen Bildgeb Verfahr 2003;175:1706–10.
8. Kuon E, Empen K, Rohde D, Dahm JB. Radiation exposure to patients undergoing percutaneous coronary interventions: are current reference values too high? Herz 2004;29:208–17.
9. Sovik E, Klow NE, Hellesnes J, Lykke J. Radiation induced skin injury after percutaneous transluminal coronary angioplasty: case report. Acta Radiol 1996;37:305–6.
10. Monaco JL, Bowen K, Tadros PN, Witt PD. Iatrogenic deep musculocutaneous injury following percutaneous coronary intervention. J Invasive Cardiol 2003;15:451–6.
11. Vano E, Gonzalez L, Guibelalde E, Fernandez JM, Ten JI. Radiation exposure to medical staff in interventional and cardiac radiology. Br J Radiol 1998;71:954–60.
12. Chong NS, Yin WS, Chan P, et al. Evaluation of absorbed radiation dose to working staff during cardiac catheterization procedures. Zhonhua Yi Xue Za Zhi 2000;63:816–21.
13. The CEC Council Directive 97/43/Euratom of 30 June 1997. Article 4: on health protection of individuals against the dangers of ionizing radiation in relation to medical exposure. Euratom Gazette 1997; L180:22–7.
14. Renaud L. A 5-year follow up of the radiation exposure to in-room personnel during cardiac catheterization. Health Phys 1992;62:10–5.
15. Valentin J. Avoidance of radiation injuries from medical interventional procedures. Ann ICRP 2000;30:7–67.
16. Kuon E, Niederst PN, Dahm JB. Usefulness of rotational spin for coronary angiography in patients with advanced renal insufficiency. Am J Cardiol 2002;90:369–73.
17. Kuon E, Dorn C, Schmitt M, Dahm JB. Radiation dose reduction in invasive cardiology by restriction to adequate instead of optimized picture quality. Health Phys 2003;84:626–31.

18. Padovani R, Bernardi G, Malisan MR, Vano E, Morocutti G, Fioretti PM. Patient dose related to the complexity of interventional cardiology procedures. Radiat Prot Dosimetry 2001;94:189–92.
19. Kuon E, Dahm JB, Schmitt M, Glaser C, Gefeller O, Pfahlberg A. Time of day influences patient radiation exposure from percutaneous cardiac interventions. Br J Radiol 2003;76:189–91.
20. Kuon E, Dahm JB. Effective training in radiation attenuating techniques requires long-term cardiology fellowship supervision. Eur J Allied Health 2002;3:20–5.
21. Kottou S, Neofotistou V, Tsapaki V, Lobotessi H, Manetou A, Molfet MG. Personnel doses in haemodynamic units in Greece. Radiat Prot Dosimetry 2001;94:121–4.
22. Watson RM. Radiation exposure: clueless in the cath lab, or sayonara ALARA. Cathet Cardiovasc Diagn 1997;42:126–7.
23. Brateman L. Radiation safety considerations for diagnostic radiology personnel: the AAPM/RSNA physics tutorial for residents. Radiographics 1999;19:1037–55.
24. Kuon E, Schmitt M, Dahm JB. Significant reduction of radiation exposure to operator and staff during cardiac interventions by analysis of radiation leakage and improved lead shielding. Am J Cardiol 2002;89:44–9.
25. Kuon E, Birkel J, Schmitt M, Dahm JB. Radiation exposure benefit of a lead cap in invasive cardiology. Heart 2003;89:1205–10.
26. Kuon E, Günther M, Gefeller O, Dahm JB. Standardization of occupational dose to patient DAP enables reliable assessment of radiation-protection devices in invasive cardiology. Rofo Fortschr Geb Rontgenstr Neuen Bildgeb Verfahr 2003;175:1545–50.
27. Vano E. Radiation exposure to cardiologists: how it could be reduced. Heart 2003;89:1123–4.
28. Pitney MR, Allan RM, Giles RW, et al. Modifying fluoroscopic view reduces operator exposure during coronary angioplasty. J Am Coll Cardiol 1994;24:1660–3.
29. Williams JR. Scatter dose estimation based on dose-area product and the specification of radiation barriers. Br J Radiol 1996;69:1032–7.
30. Marshall NW, Faulkner K. The dependence of the scattered radiation dose to personnel on technique factors in diagnostic radiology. Br J Radiol 1992;65:44–9.